ARTIFICIAL AND COMPUTATIONAL INTELLIGENCE

Fault type and fault location detection in transmission lines with 6-convolutional layered CNN

Bilal GÜMÜŞ[1] , Heybet KILIÇ[2] , Cem HAYDAROĞLU[1]* , and Ulvi Yusuf BUTAKIN[3]

[1] Electrical and Electronics Engineering Department, Faculty of Engineering, Dicle University, Diyarbakır 21280, Turkey
[2] Electric Power and Energy Department, Dicle University, Diyarbakır 21280, Turkey
[3] SCADA System and DMS Manager, Dicle Electricity Distribution Inc., Diyarbakır, Turkey

Abstract. In this article, we propose a data-driven method for short-circuit fault detection in transmission lines that exploits the capabilities of convolutional neural networks (CNNs). CNNs, a class of deep feedforward neural networks, can autonomously detect different features from data, eliminating the need for manual intervention. To mitigate the effects of noise and increase network robustness, we present a CNN architecture with six convolutional layers. The study uses a single busbar power system model developed with the PSCAD simulation program to evaluate the performance of the proposed method. The proposed CNN method is also compared with machine learning methods such as LSTM, SVM and ELM. Our results show a high success rate of 98.4% across all fault impedances, confirming the effectiveness of the proposed CNN methods in accurately detecting short-circuit faults based on current and voltage measurements.

Keywords: PSCAD; CNN; style; 6-convolutional layered CNN; fault detection.

1. INTRODUCTION

The integration of renewable energy sources, electric vehicles, and energy storage systems into power transmission networks has significantly increased their complexity [1, 2]. This heightened complexity renders power systems highly intensive enterprises, thereby elevating the risk of fault occurrences within transmission networks. Such failures not only disrupt power transmission but also inflict substantial economic damage on national economies [3]. According to the 2020 electricity losses report by the Council of European Energy Regulators (CEER), electricity losses in 18 European countries ranged between 2% and 9% from 2012 to 2018 [4]. Among these transmission system faults, 70% are single-phase ground faults. Additionally, three-phase earth faults are the most hazardous, and the occurrence of two-phase faults and two-phase earth faults, which are notably difficult to detect, also poses significant challenges [5–8].

Faults in transmission systems result in excessive current flow, power quality deterioration, and voltage drops. These issues can also lead to electrical fires, equipment loss, and life-threatening situations for personnel, adversely affecting the national economy [9]. According to the 2021 Electricity Security report, medium-sized and large commercial-industrial consumers face an instantaneous cost of 190.70$ per kWh due to outages [10]. Therefore, it is imperative to promptly detect, classify, and eliminate outages to mitigate these adverse effects.

Fault detection utilizes fault data from the literature, necessitating the extraction of distinctive features from this data. Various feature extraction methods are well-documented. Revati Godse and Sunil Bhat [11] extracted features from faulty current signals using the mathematical morphology (MM) method. Pathirikkat Gopakumar *et al*. [12] employed the Park transform and fast Fourier transform (FFT) using fault current and voltage phase angles. Das *et al*. [13] used the fast frequency S-transform method for extracting faulty current signals. Ananthan *et al*. [14] applied discrete wavelet rotation to current signals to extract features. Rathore and Shaik [15] utilized the wavelet transform on faulty current signals for feature extraction. In the study by Salehi and Namderi [16], the phase modal transform method was used to extract features from faulty current signals. Ranjbar and Jamali [17] extracted features from stream and revenue signals using the wavelet packet transform method. Malhotra *et al*. [18] extracted features from current and voltage data using the discrete wavelet transform method.

In the literature, after extracting distinguishing features, fault detection is performed using a classification algorithm. Ranjbar and Jamali employed the random forest (RF) method for fault diagnosis using fault currents and signals [17]. Swetapadma *et al*. used the decision tree (DT) method for diagnosing faults with fault current signals, although this method has the disadvantage of slow learning time [19]. Studies [20] and [21] utilized artificial neural networks (ANNs) for fault diagnosis; however, this method is not accurate for large training datasets. In the study by Papia Ray and In Mishra, support vector machines (SVMs) were used for fault detection, though this method is sensitive to parameter selection [22]. Aida Asadi Majd *et al*. diagnosed faults using the k-nearest neighbor (KNN) method with fault current signals, but this method is sensitive to noise [23].

*e-mail: cem.haydaroglu@dicle.edu.tr

B. Gümüş, H. Kılıç, C. Haydaroğlu, and U. Y. Butakın

Upon examining the literature, it becomes evident that finding a combination of a specific feature extraction technique and a particular classification model is challenging, despite the good classification results obtained with the aforementioned models. Consequently, evaluating the performance of different classification models can be time-consuming.

In this study, we first created a model using the single busbar system in power systems computer-aided design (PSCAD) software. A dataset was generated by capturing fault data from this model. We then propose a new method for fault detection in power transmission systems based on convolutional neural networks (CNN) with 6 convolutional layers, utilizing current measurements. Finally, the success of the proposed CNN system is compared with the long short term memory (LSTM), the support vector machine (SVM) and the extreme learning machine (ELM) methods, which are the most widely used machine learning algorithms in the literature. The comparisons were made on the same data set.

The contributions of this study are as follows:

- In previous studies, MATLAB was generally used for the implementation of the single busbar distribution system. Compared to MATLAB, PSCAD offers numerous advantages in modeling power systems, particularly in terms of speed and model accuracy, as it is specifically designed for power systems. Due to these features, the PSCAD program was utilized for simulation in this study.
- The proposed CNN method addresses issues such as long learning times, large computational resource requirements, quadratic programming complexities, and noise sensitivity.

2. FAULT-DIAGNOSIS METHOD FOR SINGLE TRANSMISSION LINES

In this study, a single busbar model was initially developed using the PSCAD simulation program. Subsequently, a dataset was generated by simulating various fault scenarios.

2.1. Simulation model

The single line diagram of the power system used in this study is shown in Fig. 1. The transmission line is represented in PSCAD/EMTDC using the Bergeron line model, with an ohmic-inductive load applied. The Bergeron model represents the inductance (L) and capacitance (C) elements in a distributed manner, which makes it suitable for accurately modeling the fundamental frequency. This is particularly beneficial for load flow and protection studies, where the fundamental frequency load is
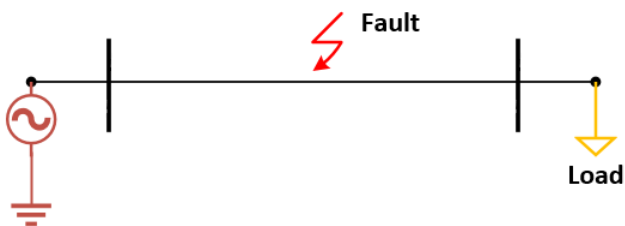
the primary concern. Additionally, the Bergeron model is computationally less intensive compared to frequency-dependent models. It allows for quicker simulations without sacrificing significant accuracy for the fundamental frequency, which was essential given our focus on relay studies and the need for efficient computation. Moreover, the Bergeron model is appropriate when detailed frequency-dependent data is not available or when a simpler model is sufficient to meet the study objectives (PSCAD). he sampling frequency used in the PSCAD simulation for this study is 3.6 kHz. The power system parameter values are provided in Table 1.

Table 1
Power system parameters

Frequency (Hz)	50
Nominal Source voltage	230 kV
Load	100 kW + 10 kVAR
Line length	300 km
Positive sequence resistance (ohm/km)	0.0275
Positive sequence inductance (ohm/km)	0.3159
Positive sequence capacitance (Mohm*m)	244.20
Zero sequence resistance (ohm/km)	0.275
Zero sequence inductance (ohm/km)	1.087
Zero sequence capacitance (Mohm*m)	373.413

The accuracy of a classification algorithm depends on a sufficient amount of data for training and testing. Therefore, it is essential to prepare a large dataset representing various faults and system conditions. The multi-run component of the PSCAD software facilitates the creation of such large datasets. By using this component, fault resistance and "fault inception angle can be set as variable parameters in PSCAD. The generated data is stored using the output file option in the PSCAD project setup [24].

The PSCAD model is shown in Fig. 2. The three-phase fault model depicted in Fig. 2 is constructed to simulate a short-circuit fault in the transmission line. With this model, ground impedance, fault type, and fault inception angle can be determined. The model was rigorously tested using a comprehensive dataset to ensure its accuracy and reliability [25]. Specifically, we generated 390 different fault scenarios, which were created by varying several parameters:

- **Fault locations:** 30 distinct locations along the transmission line at 10 km intervals.
- **Fault resistances:** 0 ohm, 10 ohm, 30 ohm, 50 ohm, and 100 ohm.
- **Fault inception angles:** Various angles including 0, 45, 60, 90, 135, 170, 225, 260, and 320 degrees.
- **Fault types:** A range of fault types such as AG, BG, CG, AB, AC, BC, ABG, ACG, BCG, and ABC.

These scenarios were simulated in PSCAD, which allowed us to test the model under diverse conditions, ensuring its robustness and effectiveness in detecting and classifying different

Fig. 1. Transmission line model

2

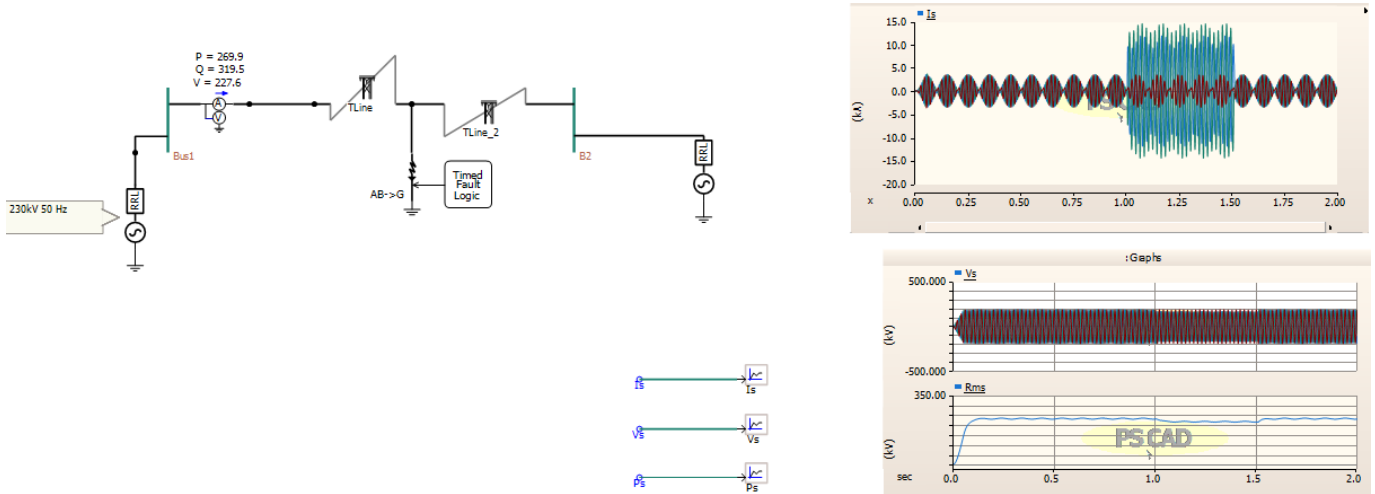*Bull. Pol. Acad. Sci. Tech. Sci.*, vol. 72, no. 5, e151047, 2024

Fig. 2. PSCAD model

types of faults. Moreover, The fault signals in our study were recorded for a duration of 0.1 seconds, capturing both pre-fault and post-fault conditions to ensure a comprehensive analysis. The recording started 0.05 seconds before the fault occurrence, providing a clear view of the system behavior before, during, and after the fault event.

2.2. Convolutional neural network (CNN)

Convolutional neural networks (CNN) were first developed by Yann LeCun for recognizing digital handwritten digits [26, 27]. The original model featured smaller layers compared to modern CNNs, which now have higher-dimensional layers and weights. It consisted of successive convolution and subsampling layers, totaling four layers (2 convolutional and 2 subsampling), followed by two fully connected layers. With advancements in hardware technologies, larger layers have been proposed. For instance, Krizhevsky et al. used a structure consisting of 5 convolutional layers (5C), 3 subsampling layers (3S), 2 fully connected layers (2FC), and 1 Softmax layer to classify a 1000-class dataset in the ImageNet competition [28]. Over the past decade, numerous CNN models featuring various architectures have been introduced. Unlike traditional feature extraction methods, CNNs utilize different filter structures to extract features that maximize distinguishability from the signal or image. The typical layers in a CNN include Convolution, Subsampling, Dropout, Fully Connected, and Softmax.

Convolution layer: In the convolution layer, randomly generated filters are applied to the input signal to extract its distinctive features. The sizes and characteristics of these filters vary. After filtering the input signal, activation maps are produced, with each activation map representing a different attribute of the signal.

$$b[n] = \sum_{k=1}^{l} x[n] \times w[k]. \tag{1}$$

Here, $x[n]$ denotes the n-dimensional input signal, $w[k]$ denotes the k-dimensional filter, and $b[n]$ the output signal to be obtained.

Figure 3 shows the convolution operation applied to a one-dimensional signal. $x[n]$ denotes n-length input signal, $w[k]$ denotes k-length filter applied to input signal. $b[n]$ denotes the output signal obtained as a result of convolution. The process is designed to take the average of every 5 elements of a signal given as input to the system. Equation (2) is an equation expressed with symbols commonly used in the literature used to calculate the length of the output obtained as a result of the process expressed in the figure

$$\frac{w - f + 2p}{s} + 1, \tag{2}$$

where w is the dimensions of the input image, f is the length of the filter applied to the input image, p is the amount of expansion in terms of no loss from the input image, and s is how many steps the filter will advance.
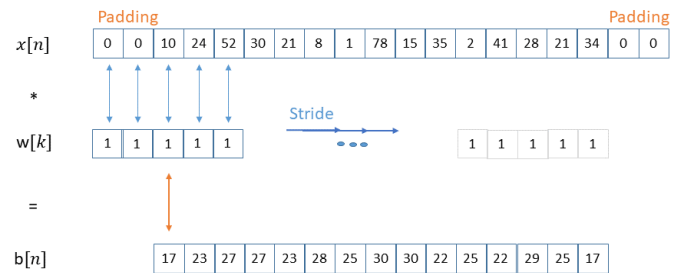

Fig. 3. An image expressing the convolution operation applied to a one-dimensional signal

Subsampling layer: This layer is applied to the activation maps obtained from the previous convolution layer, reducing the data size. This reduction decreases processing costs in subsequent layers and initiates the extraction of higher-level features. Subsampling operations can be either max-pooling or average-pooling.

Dropout: In this layer, operation costs are reduced by eliminating neurons (nodes) from the activation maps that do not contribute to discrimination. This process also enhances focus on neurons that provide discrimination in the next layer.

B. Gümüş, H. Kılıç, C. Haydaroğlu, and U. Y. Butakın
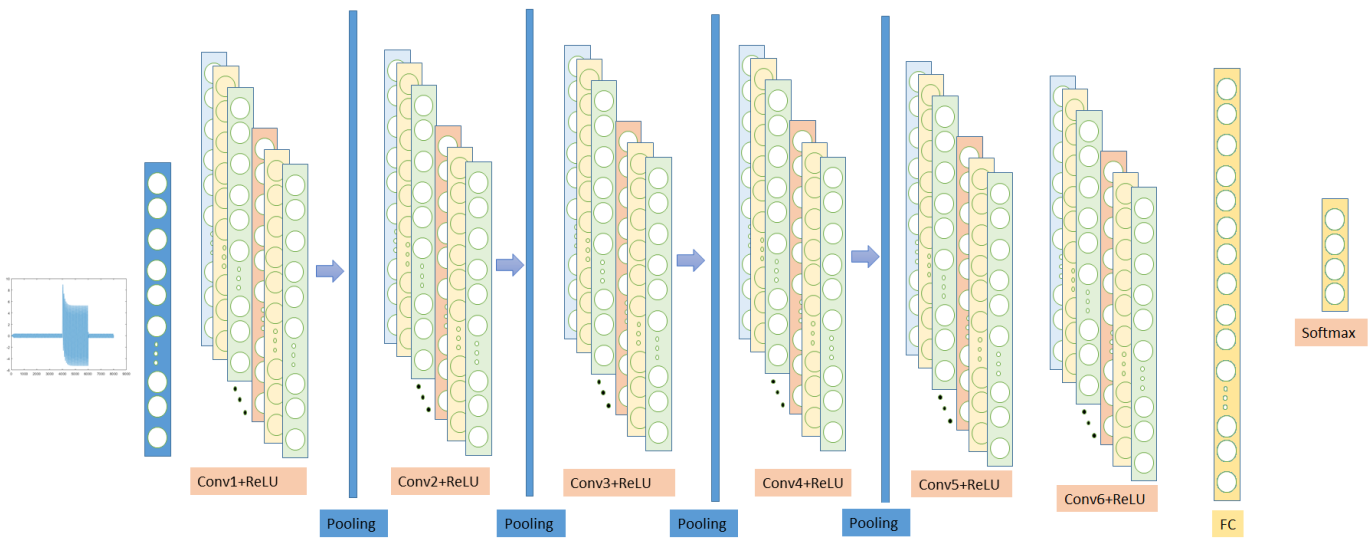
Fig. 4. In this proposed study, (custom) convolutional neural networks applied to the input signal. CNN architecture consists of 6 Convolution, 4 Subsampling and 1 FC and 1 Softmax layers

Fully connected layer: After applying a series of convolution and subsampling layers, the data is vectorized before classification in this layer. A standard CNN architecture typically includes multiple fully connected layers, ensuring that the weights of neurons contributing most to classification success are increased. Dropout can also be performed in these layers to eliminate neurons that do not contribute to the result, further reducing operation costs.

Softmax layer: Classification is performed in this layer, which contains as many neurons as the total number of classes in the dataset. Each neuron has a value in the range of 0–1, with the neuron having the maximum value being considered the output.

Figure 4 illustrates the model applied in this proposed study. The model consists of 6 convolutional layers, 4 subsampling layers, 1 fully connected layer, and 1 Softmax layer. The convolutional layers apply 32 5-dimensional, 64 3-dimensional, 128 5-dimensional, 256 3-dimensional, 256 7-dimensional, and 32 3-dimensional filters to the relevant signals, respectively. Each subsampling layer uses a stride value of 2, halving the resulting output signal. The ReLU activation function is used in the model [29]. In the final stage, to obtain a one-dimensional vector of length 512, the dense layer is followed by Softmax layers with neurons equal to the number of classes (four) to classify.

3. SIMULATION RESULTS AND DISCUSSION

PSCAD/EMTDC is the industry-standard proprietary simulation tool for analyzing the transient behavior of electrical networks. This advanced simulation program offers a comprehensive graphical user interface, real-time model applications, runtime control, and result analysis within a single integrated environment. It enables the precise and efficient modeling of FACTS and HVDC systems and supports both AC and DC

power plant components and controls. In our study, we leveraged these advantages to create a realistic application using the PSCAD/EMTDC Simulator [30, 31].

Figure 5 shows the accuracy rate of the CNN algorithm in fault detection in comparison with the long short term memory (LSTM), support vector machine (SVM) and extreme learning machine (ELM) methods. CNN was found to predict faults with the highest accuracy for all fault impedances compared to these methods. Using the raw data, the fault impedance of 0 ohms was classified by the CNN method with 100% success. When the fault impedance was increased to 30 ohms, the CNN algorithm showed 99.75% classification success, and when the fault impedance was increased to 50 ohms, the CNN algorithm showed 99.5% success. Finally, when the fault impedance was increased to 100 ohms, the CNN algorithm detected the fault at
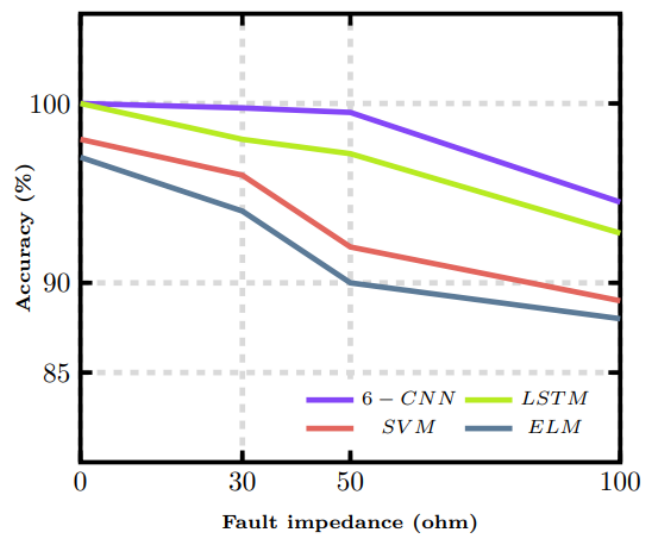
Fig. 5. The fault detection accuracy of different methods

4

Bull. Pol. Acad. Sci. Tech. Sci., vol. 72, no. 5, p. e151047, 2024

a rate of 94.5%. The LSTM method achieved 100% accuracy in 0 ohm fault impedance and 92.77% accuracy in 100 ohm fault impedance. The SVM method achieved 98% accuracy in 0 ohm fault impedance, and 89% accuracy in 100 ohm fault impedance. The ELM method achieved 97% accuracy in 0 ohm fault impedance, and 88% accuracy in 100 ohm fault impedance. It was found that the CNN method can be highly accurate for fault detection even at high fault impedances.

In order to estimate the fault location, a dataset was prepared by creating 50 faults for different fault types at locations approximately 90, 50 and 10 km from the supply busbar. The success of CNN, LSTM, SVM and ELM was analysed on this data set. The results obtained for the different fault types are shown in Tables 3–6. The tables show the number of false detections, the distance of the false detection from the actual fault location and the average error value for different line lengths and fault impedances for the analysed methods. At a distance of more than 0.5 km from the actual fault location, there are no false detections. For this reason, the distances to the actual fault location for false detections were classified into 3 categories between 0 and 0.5 km. These categories are 0–0.1 km, 0.2–0.3 km and 0.4–0.5 km from the actual fault location. Accurate fault location determinations indicate that the fault location can be determined with an accuracy of 1 km.

Table 2 shows the fault location results for 3-phase faults. Analysing Table 3, for example, 27 out of 50 faults with a fault impedance of 100 Ohm at a distance of 90 km from the supply busbar were correctly detected, while 11 faults with a distance error between 0 and 0.1 km, 8 faults with a distance error between 0.2 and 0.3 km and 3 faults with a distance error between 0.4 and 0.5 km were incorrectly detected. CNN is the most successful detection method compared to the other methods analysed. The number of incorrect detections for the location ranges from 21 to 26 for the CNN, 23 to 29 for the LSTM, 24 to 36 for the SVM and 34 to 42 for the ELM. For the 3-phase short-circuit fault, the average error range of the CNN method varies between 0.19% and 0.23% for these different distances and fault impedances. For the same type of fault, the average error range of the LSTM method varies between 0.21% and 0.25%, the average error range of the SVM method varies between 0.23% and 0.27% and the average error range of the ELM method varies between 0.25% and 0.30%.

Table 3 shows the fault location results for single-phase ground faults. The number of incorrect detections for the location ranges from 21 to 29 for the CNN, 24 to 34 for the LSTM, 30 to 37 for the SVM and 37 to 43 for the ELM. The average error range of the CNN method for single-phase earth faults varies between 0.18% and 0.27% for different distances and fault impedances. For the same type of fault, the average error range varies between 0.22% and 0.30% for the LSTM method, between 0.23% and 0.33% for the SVM method and between 0.25% and 0.37% for the ELM method. The CNN method was found to give the best results.

Table 4 shows the fault location results for two phase faults. The number of incorrect detections for the location ranges from 19 to 26 for the CNN, 21 to 30 for the LSTM, 24 to 33 for the SVM and 27 to 38 for the ELM. The average error range of the

Table 2
3 Phase fault location results

	Ohm	Line	Number of fault detections			Average error range %
			0–0.1 km	0.2–0.3 km	0.4–0.5 km	
6-CNN	100	90	11	8	4	0.20
		50	13	5	4	0.23
		10	13	5	3	0.23
	50	90	11	6	3	0.21
		50	12	10	4	0.23
		10	13	6	2	0.22
	0	90	11	11	4	0.20
		50	10	9	3	0.23
		10	14	8	3	0.20
LSTM	100	90	12	9	5	0.22
		50	15	6	5	0.25
		10	15	6	4	0.26
	50	90	12	7	4	0.24
		50	13	11	5	0.26
		10	15	7	2	0.24
	0	90	12	12	5	0.22
		50	11	10	4	0.25
		10	16	9	4	0.23
SVM	100	90	15	11	7	0.24
		50	16	7	8	0.26
		10	17	8	7	0.28
	50	90	14	8	7	0.27
		50	15	13	8	0.28
		10	16	11	7	0.26
	0	90	14	14	8	0.24
		50	12	12	5	0.27
		10	18	11	6	0.26
ELM	100	90	17	13	9	0.26
		50	18	9	10	0.28
		10	19	11	9	0.30
	50	90	16	10	9	0.29
		50	17	15	10	0.30
		10	18	12	11	0.28
	0	90	16	15	9	0.27
		50	13	14	7	0.30
		10	19	13	8	0.29

CNN method for single-phase earth faults varies between 0.20% and 0.23% for different distances and fault impedances. For the same type of fault, the average error range varies between 0.22% and 0.26% for the LSTM method, between 0.24% and 0.27% for the SVM method and between 0.25% and 0.29% for the ELM method. The CNN method was found to give the best results.

Table 5 shows the fault location results for two phase-ground faults. The number of incorrect detections for the location ranges from 20 to 25 for the CNN, 23 to 28 for the LSTM, 27 to 33

B. Gümüş, H. Kılıç, C. Haydaroğlu, and U. Y. Butakın

Table 3

Single phase-ground fault location results

	Ohm	Line	Number of fault detections			Average error range %
			0–0.1 km	0.2–0.3 km	0.4–0.5 km	
6-CNN	100	90	12	8	5	0.21
		50	11	7	3	0.22
		10	11	7	4	0.22
	50	90	16	8	3	0.22
		50	11	10	5	0.27
		10	15	7	7	0.23
	0	90	12	9	2	0.18
		50	15	6	3	0.21
		10	13	8	4	0.19
LSTM	100	90	13	9	6	0.24
		50	12	8	4	0.24
		10	12	8	5	0.25
	50	90	18	9	4	0.25
		50	12	11	6	0.30
		10	17	8	9	0.26
	0	90	13	10	2	0.20
		50	17	7	4	0.23
		10	15	9	5	0.22
SVM	100	90	15	11	9	0.31
		50	14	10	6	0.32
		10	14	10	7	0.33
	50	90	20	10	6	0.28
		50	14	13	8	0.34
		10	18	9	10	0.29
	0	90	15	11	5	0.23
		50	19	9	7	0.25
		10	17	11	8	0.24
ELM	100	90	17	13	11	0.33
		50	16	12	9	0.35
		10	16	13	9	0.36
	50	90	21	11	8	0.31
		50	17	14	10	0.37
		10	20	11	12	0.32
	0	90	17	13	7	0.26
		50	21	11	9	0.27
		10	19	12	10	0.25

Table 4

Two phase fault location results

	Ohm	Line	Number of fault detections			Average error range %
			0–0.1 km	0.2–0.3 km	0.4–0.5 km	
6-CNN	100	90	10	10	4	0.20
		50	14	7	5	0.22
		10	13	7	3	0.22
	50	90	13	5	3	0.21
		50	11	9	2	0.23
		10	10	8	2	0.22
	0	90	10	7	2	0.20
		50	11	6	3	0.23
		10	10	7	2	0.21
LSTM	100	90	11	11	5	0.22
		50	16	8	6	0.25
		10	15	8	4	0.25
	50	90	15	6	4	0.24
		50	12	10	2	0.26
		10	11	9	2	0.25
	0	90	11	8	2	0.23
		50	12	7	4	0.25
		10	11	8	2	0.23
SVM	100	90	12	12	6	0.25
		50	17	9	7	0.27
		10	16	10	5	0.26
	50	90	16	7	6	0.25
		50	13	12	3	0.27
		10	12	10	4	0.27
	0	90	12	9	3	0.24
		50	13	8	5	0.26
		10	12	9	4	0.24
SVM	100	90	13	14	7	0.27
		50	18	11	9	0.28
		10	17	11	6	0.29
	50	90	17	9	8	0.26
		50	14	13	3	0.28
		10	13	11	5	0.28
	0	90	13	10	4	0.26
		50	15	9	4	0.27
		10	14	11	5	0.25

for the SVM and 28 to 36 for the ELM. The average error range of the CNN method for single-phase earth faults varies between 0.19% and 0.24% for different distances and fault impedances. For the same type of fault, the average error range varies between 0.23% and 0.28% for the LSTM method, between 0.27% and 0.33% for the SVM method and between 0.28% and 0.36% for the ELM method. The CNN method was found to give the best results.

In this study, fault types in distribution systems are detected and classified using the 6 Evolution Layered CNN method. At the same time, the success of the CNN method is compared with other machine learning methods. For high impedance faults that occur in distribution lines, fault detection becomes difficult and the accuracy of the methods decreases. Table 6 shows MAT-LAB simulations from the literature and the accuracy of different methods in detecting literature in comparison with the

6

Bull. Pol. Acad. Sci. Tech. Sci., vol. 72, no. 5, p. e151047, 2024

Table 5

Two phase-ground fault location results

	Ohm	Line	Number of fault detections			Average error range %
			0–0.1 km	0.2–0.3 km	0.4–0.5 km	
6-CNN	100	90	12	5	4	0.19
		50	11	6	3	0.22
		10	12	8	4	0.22
	50	90	13	7	4	0.23
		50	12	6	3	0.23
		10	13	8	2	0.22
	0	90	10	10	1	0.20
		50	10	11	4	0.24
		10	14	5	3	0.20
LSTM	100	90	13	6	5	0.21
		50	12	7	4	0.25
		10	13	9	5	0.25
	50	90	15	8	5	0.26
		50	13	7	4	0.26
		10	15	9	2	0.25
	0	90	11	11	1	0.22
		50	11	12	5	0.27
		10	16	6	4	0.23
SVM	100	90	14	7	6	0.23
		50	13	8	5	0.27
		10	15	10	7	0.27
	50	90	16	9	6	0.28
		50	14	8	5	0.29
		10	17	11	5	0.27
	0	90	12	13	5	0.24
		50	13	14	6	0.27
		10	17	7	5	0.25
ELM	100	90	15	9	7	0.24
		50	14	9	5	0.28
		10	16	11	8	0.29
	50	90	17	10	7	0.29
		50	14	9	6	0.31
		10	16	12	8	0.29
	0	90	13	14	8	0.24
		50	14	15	7	0.28
		10	16	9	6	0.29

proposed method. The simulations performed with MATLAB are not in real time, which increases the error probability of the simulations. Analysing the method using datasets obtained from real-time simulations will provide more accurate results. The data required to test the CNN method proposed in this study was obtained by real-time simulation of a single busbar system modelled in PSCAD. In particular, the real-time model implementations, runtime checks and analysis of the results are obtained from the perspective of looking at modern distribution systems from the workspaces thanks to a simulation program that provides a single integrated data. The real-time migration of the model increased the constraint. In this case, the fault type was detected with 98.5% accuracy using the CNN method. The proposed 6-layer CNN method was found to give better results than LSTM, SVM and ELM methods.

4. CONCLUSIONS

In this study, data were obtained for single phase ground fault, 2 phase ground fault, phase phase fault, 3 phase short circuit fault conditions at 0 ohm, 30 ohm, 50 ohm and 100 ohm fault short circuit resistances, different angle values and different kms in single busbar power system modelled in PSCAD. A CNN method with 6 convolutional layers is presented to detect short circuit faults of different resistances and types. The proposed CNN method is also compared with LSTM, SVM and ELM methods. Data obtained from the system modelled in PSCAD were used to test the accuracy of the method. The data was not pre-processed. The fault location distance estimation algorithm based on the data obtained from the PSCAD real-time simulation results works satisfactorily in all scenarios. The simulation results show that the average distance estimation error never exceeds 0.37% and most distance errors are located with an error of less than 0.24% for all methods.

In this study, where raw data was applied, the CNN algorithm shows the highest accuracy. It was classified in the CNN algorithm at 0 ohm fault impedance with 100% success. When the fault impedance was increased to 30 ohms, the CNN algorithm showed 99.75% classification success, and when the fault impedance was increased to 50 ohms, the CNN algorithm showed 99.5% success. Finally, when the fault impedance was increased to 100 ohms, the CNN algorithm detected the fault very accurately even at high fault impedances with a rate of 94.5%. In this study, high impedance faults, especially those that are difficult to predict, were detected very accurately. In addition, 98.5% of the fault types were correctly identified.

Table 6

Compared with other studies in the literature

	Topology	Data acquisition	Implementation	Algorithm	Accuracy (%)
[32]	single transmission line model	3 phase current and voltage data	MATLAB	CSAE	92.2%
[33]	single transmission line model	3 phase current signals were used	MATLAB	SVM classifiers	98.5%
[34]	single transmission line model	3 phase current and voltage data	MATLAB	CNN	99%
[35]	single transmission line model	3 phase current signals were used	MATLAB	k-means clustering	99.5%
Proposed method	single transmission line model	3 phase current signals were used	PSCAD	6-convolution layered CNN	98.5%

Bull. Pol. Acad. Sci. Tech. Sci., vol. 72, no. 5, p. e151047, 2024

7

ACKNOWLEDGEMENTS

REFERENCES

[1] Y.M. Nsaif, M.S.H. Lipu, A. Ayob, Y. Yusof, and A. Hussain, "Fault detection and protection schemes for distributed generation integrated to distribution network: Challenges and suggestions," *IEEE Access*, vol. 9, pp. 142 693–142 717, 2021, doi: 10.1109/ACCESS.2021.3121087.

[2] A. Silos-Sanchez, R. Villafafila-Robles, and P. Lloret-Gallego, "Novel fault location algorithm for meshed distribution networks with ders," *Electr. Power Syst. Res.*, vol. 181, p. 106182, 2020.

[3] H. Kilic, B. Gumus, and M. Yilmaz, "Fault detection in photovoltaic arrays: a robust regularized machine learning approach." *DYNA-Ingeniería e Industria*, vol. 95, no. 6, pp. 622–628, 2020, doi: 10.6036/9856.

[4] Council of European Energy Regulators, "2nd ceer report on power losses," 2020. [Online]. Available: https://www.ceer.eu/documents/104400/-/-/fd4178b4-ed00-6d06-5f4b-8b87d630b060

[5] S.A. Aleem, N. Shahid, and I.H. Naqvi, "Methodologies in power systems fault detection and diagnosis," *Energy Syst.*, vol. 6, pp. 85–108, 2015.

[6] Y.Q. Chen, O. Fink, and G. Sansavini, "Combined fault location and classification for power transmission lines fault diagnosis with integrated feature extraction," *IEEE Trans. Ind. Electron.*, vol. 65, no. 1, pp. 561–569, 2018, doi: 10.1109/TIE.2017.2721922.

[7] S. Gururajapathy, H. Mokhlis, and H. Illias, "Fault location and detection techniques in power distribution systems with distributed generation: A review," *Renew. Sust. Energ. Rev.*, vol. 74, pp. 949–958, 2017.

[8] C. Haydaroğlu and B. Gümüş, "Fault detection in distribution network with the Cauchy-M estimate – RVFLN method," *Energies*, vol. 16, no. 1, 2023.

[9] H. Haes Alhelou, M. E. Hamedani-Golshan, T.C. Njenda, and P. Siano, "A survey on power system blackout and cascading events: Research motivations and challenges," *Energies*, vol. 12, no. 4, p. 682, 2019, doi: 10.3390/en12040682.

[10] "Analytical frameworks for electricity security," International Energy Agency, Tech. Rep., 2021. [Online]. Available: https://www.iea.org/reports/analytical-frameworks-for-electricity-security

[11] R. Godse and S. Bhat, "Mathematical morphology-based feature-extraction technique for detection and classification of faults on power transmission line," *IEEE Access*, vol. 8, pp. 38 459–38 471, 2020, doi: 10.1109/ACCESS.2020.2975431.

[12] P. Gopakumar and D.K. Mohanta, "Adaptive fault identification and classification methodology for smart power grids using synchronous phasor angle measurements," *IET Gener. Transm. Distrib.*, vol. 9, pp. 133–145, 2015.

[13] P.K. Dash, S. Das, and J. Moirangthem, "Distance protection of shunt compensated transmission line using a sparse s-transform," *IET Gener. Transm. Distrib.*, vol. 9, pp. 1264–1274, 2015.

[14] S.N. Ananthan, R. Padmanabhan, R. Meyur, B. Mallikarjuna, M.J.B. Reddy, and D.K. Mohanta, "Real-time fault analysis of transmission lines using wavelet multi-resolution analysis based frequency-domain approach," *IET Sci. Meas. Technol.*, vol. 10, pp. 693–703, 2016.

[15] B. Rathore and A.G. Shaik, "Wavelet-alienation based transmission line protection scheme," *IET Gener. Transm. Distrib.*, vol. 11, pp. 995–1003, 2017.

[16] M. Salehi and F. Namdari, "Fault classification and faulted phase selection for transmission line using morphological edge detection filter," *IET Gener. Transm. Distrib.*, vol. 12, pp. 1595–1605, 2018.

[17] S. Ranjbar and S. Jamali, "Fault detection in microgrids using combined classification algorithms and feature selection methods," in *2019 International Conference on Protection and Automation of Power System (IPAPS)*, 2019, pp. 17–21, doi: 10.1109/IPAPS.2019.8641871.

[18] A. Malhotra, O. P. Mahela, and H. Doraya, "Detection and classification of power system faults using discrete wavelet transform and rule based decision tree," in *2018 International Conference on Computing, Power and Communication Technologies (GUCON)*, 2018, pp. 142–147, doi: 10.1109/GUCON.2018.8674922.

[19] A. Swetapadma and A. Yadav, "A novel decision tree regression-based fault distance estimation scheme for transmission lines," *IEEE Trans. Power Deliv.*, vol. 32, no. 1, pp. 234–245, 2017, doi: 10.1109/TPWRD.2016.2598553.

[20] A. Yadav and Y. Dash, "An overview of transmission line protection by artificial neural network: Fault detection, fault classification, fault location, and fault direction discrimination," *Adv. Artif. Neural Syst.*, 2014, doi: 10.1155/2014/230382.

[21] M. Jamil, K.S. Sharma, and R. Singh, *SpringerPlus*, vol. 4, p. 334.

[22] P. Ray and D.P. Mishra, "Support vector machine based fault classification and location of a long transmission line," *Eng. Sci. Technol. Int. J.*, vol. 19, no. 3, pp. 1368–1380, 2016.

[23] A.A. Majd, H. Samet, and T. Ghanbari, "k-nn based fault detection and classification methods for power transmission systems," *Prot. Control Mod. Power Syst.*, vol. 2, p. 32, 2017, doi: 10.1186/s41601-017-0063-z.

[24] M.H. Hairi, M.N. Kamarudin, A.S.M. Isira, M.F.P. Mohamed, and S.A. Sobri, "Modeling an overcurrent relay protection and coordination in a power system network using pscad software," *Int. J. Electr.l Eng. Appl. Sci.*, vol. 4, no. 1, 2021. [Online]. Available: https://ijeeas.utem.edu.my/ijeeas/article/view/4153

[25] M. Singh, B. Panigrahi, and R.P. Maheshwari, "Transmission line fault detection and classification," in *2011 International Conference on Emerging Trends in Electrical and Computer Technology*, 2011, pp. 15–22, doi: 10.1109/ICETECT.2011.5760084.

[26] Y. Lecun, L. Bottou, Y. Bengio, and P. Haffner, "Gradient-based learning applied to document recognition," *Proc. IEEE*, vol. 86, no. 11, pp. 2278–2324, 1998, doi: 10.1109/5.726791.

[27] Y. LeCun, B.E. Boser, J.S. Denker, D. Henderson, R.E. Howard, W.E. Hubbard, and L.D. Jackel, "Handwritten digit recognition with a back-propagation network," in *NIPS*, 1989.

[28] A. Krizhevsky, I. Sutskever, and G.E. Hinton, "Imagenet classification with deep convolutional neural networks," in *Advances in Neural Information Processing Systems*, F. Pereira, C. Burges, L. Bottou, and K. Weinberger, Eds., vol. 25. Curran Associates, Inc., 2012.

[29] F. Murat, O. Yildirim, M. Talo, U.B. Baloglu, Y. Demir, and U.R. Acharya, "Application of deep learning techniques for heartbeats detection using ecg signals-analysis and review," *Comput. Biol. Med.*, vol. 120, p. 103726, 2020, doi: 10.1016/j.compbiomed.2020.103726.

[30] S.-Y. Park, G.-W. Kim, J.-S. Jeong, and H.-S. Choi, "The modeling of the LC divergence oscillation circuit of a superconducting dc circuit breaker using pscad/emtdc," *Energies*, vol. 15, no. 3, p. 780, 2022, doi: 10.3390/en15030780.

[31] A.L. Nascimento, I. Yahyaoui, J.F. Fardin, L.F. Encarnação, and F. Tadeo, "Modeling and experimental validation of a pem fuel cell in steady and transient regimes using pscad/emtdc software," *Int. J. Hydrog. Energy*, vol. 45, no. 55, pp. 30 870–30 881, 2020, doi: 10.1016/j.ijhydene.2020.04.184.

[32] K. Chen, J. Hu, and J. He, "Detection and classification of transmission line faults based on unsupervised feature learning and convolutional sparse autoencoder," *IEEE Trans. Smart Grid*, vol. 9, pp. 1748–1758, 2017.

[33] M. Coban and S.S. Tezcan, "Detection and classification of short-circuit faults on a transmission line using current signal," *Bull. Pol. Acad. Sci. Tech. Sci.*, vol. 69, no. 4, p. e137630, 2021, doi: 10.24425/bpasts.2021.137630.

[34] S. Fuada, H. Shiddieqy, and T. Adiono, "A high-accuracy of transmission line faults (TLFs) classification based on convolutional neural network," *Int. J. Electron. Telecommun.*, vol. 66, no. 4, pp. 655–664, 2020, doi: 10.24425/ijet.2020.134024.

[35] A.K. Gangwar, O.P. Mahela, B. Rathore, B. Khan, H.H. Alhelou, and P. Siano, "A novel k-means clustering and weighted k-nn-regression-based fast transmission line protection," *IEEE Trans. Ind. Inform.*, vol. 17, no. 9, pp. 6034–6043, 2021, doi: 10.1109/TII.2020.3037869.

Bull. Pol. Acad. Sci. Tech. Sci., vol. 72, no. 5, p. e151047, 2024

9